Contract No.:

This manuscript has been authored by Savannah River Nuclear Solutions (SRNS), LLC under Contract No. DE-AC09-08SR22470 with the U.S. Department of Energy (DOE) Office of Environmental Management (EM).

Disclaimer:

Vibrational Spectroscopy of Uranium Tetrafluoride Hydrates

Michael A. DeVore II[†], Eliel Villa-Aleman[†], Justin B. Felder[‡], Jeongho Yeon[‡], Hans-Conrad zur Loye[‡], Matthew S. Wellons[†]*

[†]National Security Directorate, Savannah River National Laboratory, Aiken SC 29808

[‡]Department of Chemistry and Biochemistry, University of South Carolina, Columbia SC 29208

* Corresponding Author michael.devore@srnl.doe.gov

Highlights

- Characterization of UF_4 hydrates with vibrational spectroscopy (Raman and infrared spectroscopy)

Abstract

Uranium tetrafluoride (UF_4) is an important intermediate in the production of UF_6 and nuclear fuel. Historical characterization of UF_4 with Raman spectroscopy was plagued with ambiguity until the first accurate Raman spectrum was published by our group in 2016. Although generally considered to be relatively stable, UF_4 can hydrolyze to form numerous UF_4 hydrates that may play a role in future uranium waste forms. In contrast to anhydrous UF_4, the hydrates, with their OH stretch and HOH bending modes, can be spectroscopically characterized by the type and degree of water bonding in the crystal lattice, which can yield additional information about their crystal structure. Herein, vibrational spectroscopy (Raman and infrared) was used to characterize three different UF_4 hydrates: $UF_4(H_2O)_{0.33}$, $U_3F_{12}(H_2O)$, and $UF_4(H_2O)_{2.5}$. Spectra show the different hydrates vary in the number of observed bands, full-width half-maximum of the bands, and band intensity. These differences are due to varying interactions between the OH stretch and HOH bending modes with UF_4 and the polymeric UF_4 structure in the crystal lattice. These vibrational data, in combination with spectral fitting and crystallographic structures measured with powder X-ray diffraction and single crystal X-ray diffraction, provide unique details on the location of water molecules in the crystal lattice of hydrated UF_4, and provide an interesting contrast to the vibrational spectra of anhydrous UF_4.

Keywords

Vibrational spectroscopy, Raman, Infrared, UF_4, UF_4 hydrates

1.1 Introduction

Uranium fluorides are ubiquitous in the nuclear fuel cycle.[1-6] Uranium tetrafluoride (UF_4) is particularly important, as it is the most commonly used intermediate in chemical conversion processes leading to uranium metal or uranium hexafluoride (UF_6). That said, improved understanding of the structure of UF_4 and its hydrated analogs remains a key goal in multiple research fields, including nuclear nonproliferation and environmental remediation.

The earliest reports of UF_4 hydrates were by Khlopin et al. who claimed to have isolated three U^{4+} hydrates, $UF_4(H_2O)_x$ (x = ½, 1, and 2).[7,8] These compounds were synthesized by electrolytic reduction of uranyl fluoride (UO_2F_2) in aqueous hydrofluoric acid. Further characterization showed that all three were actually $UF_4(H_2O)_2$.[8] Later, Gabuda et al. published a report of two new UF_4 hydrates which included the monoclinic $UF_4(H_2O)_{4/3}$, and the orthorhombic $UF_4(H_2O)_{2.5}$.[9] The structure for $UF_4(H_2O)_{4/3}$ was determined via powder X-ray diffraction (pXRD), optical methods, and Nuclear Magnetic Resonance (NMR) spectroscopy.[10] Structural data for the orthorhombic $UF_4(H_2O)_{2.5}$ was eventually obtained by single crystal X-ray diffraction but did not appear in the open literature until 1971; many years after the compound was first reported.[11] More recently, a trinuclear U^{4+} fluoride, $U_3F_{12}(H_2O)$, was synthesized by a mild hydrothermal route and was characterized by single crystal X-ray diffraction.[3]

In 1975, Goldstein et al. examined the Raman spectra of ZrF_4, HfF_4, and CeF_4, and postulated that a three-dimensional polymeric structure existed for these molecules. Although Goldstein attempted to prove that this structure also applied to UF_4, his attempts to measure the Raman spectrum of UF_4 were hindered by significant fluorescence that overwhelmed the weak Raman signal. In 2016, our group employed multiple wavelength lasers to unambiguously measure the Raman signature of UF_4 for the first time.[12] The polymeric structure that Goldstein had suspected was confirmed by the observation of 16 bands in the Raman spectrum of UF_4. In fact, subsequent symmetry analysis of UF_4 by Miskowiec et al. has determined that as many as 42 vibrational modes should be active in UF_4 due to its complex polymeric structure.[13] Despite these advancements, little has been done to apply similar vibrational spectroscopy techniques towards the study of the hydrated analogs of UF_4, although application of these techniques can help elucidate the location of water molecules in the crystal lattice, which might help reveal more about the complex UF_4 structure. For example, band frequencies and full-width at half-maximum (FWHM) values of the water OH stretch bands can be used as a probe to indicate the type of hydrogen bonding or the presence of free OH functional groups in the crystal lattice. If present, these modes likely correlate to the complex polymeric UF_4 lattice structure. Additionally, the number of bands in the HOH bending region can indicate the number of water sites in different chemical environments. This information is key to understanding the arrangement of the atoms in the crystal lattice.

To this end, we employed Raman and IR spectroscopic methods to characterize bonding and the chemical environment for a series of uranium tetrafluoride hydrates, $UF_4(H_2O)_{2.5}$, $UF_4(H_2O)_{0.33}$, and $U_3F_{12}(H_2O)$. Spectral data are compared with crystallographic data to elucidate the origin of spectroscopic observables. All structural information within this effort was confirmed via single crystal XRD characterization or by powder XRD pattern matches to known materials. Neither the Raman nor IR spectra for these hydrates have been previously published and we provide a comprehensive comparison of these spectra with spectra of anhydrous UF_4.[14]

1.2 **Chemicals and Synthesis**

1.2.1 UF_4

Anhydrous UF_4 was purchased from International Bio-Analytical Laboratories Inc. The compound has a vibrant emerald-green color and spherical particle morphology with dimensions that range from a few microns up to thirty microns in diameter. Purity and material phase were confirmed by powder X-ray diffraction (pXRD). The pXRD pattern was consistent with UF_4 and no other crystalline materials were detectable (Powder Diffraction File [PDF] No. 01-082-2317).[15,16,17]

1.2.2 $U_3F_{12}(H_2O)$

Single crystals of $U_3F_{12}(H_2O)$ were synthesized via a previously published hydrothermal route using $UO_2(CH_3CO_2)_2 \cdot 2H_2O$, $Cu(CH_3CO_2)_2 \cdot 2H_2O$, and dilute HF.[18] Characterization of the resultant green crystals included single crystal and powder X-ray diffraction (XRD).

1.2.3 $UF_4(H_2O)_{0.33}$

Single crystals of $UF_4(H_2O)_{0.33}$ were synthesized via a mild hydrothermal route using $UO_2(CH_3CO_2)_2$ and V_2O_5 heated in a H_2O/HF mixture at 200 ˚C for 24 hrs. The product was a mixture of bright green single crystals of both $UF_4(H_2O)_{0.33}$ and $U_3F_{12}(H_2O)$. Individual crystals of $UF_4(H_2O)_{0.33}$ were isolated for subsequent analyses based on minor but consistent differences in coloration with $U_3F_{12}(H_2O)$. The crystal structure of $UF_4(H_2O)_{0.33}$ was determined via single crystal XRD. See **Tables S1-3** for detailed crystallographic information and interatomic distances.

1.2.4 $UF_4(H_2O)_{2.5}$

$UF_4(H_2O)_{2.5}$ was synthesized by mixing 0.10 g of anhydrous UF_4 in 25 ml of deionized water in a Teflon centrifuge tube at room temperature for multiple days. After 24 hours, the color of the solid turned from emerald green to blue-green. The solid was filtered, dried, and isolated as needle-like microcrystals (see SI Figure X). Multiple mixing durations were tested and the products characterized by XRD; in all instances where mixing was between 48-144 hours, the filtered product yielded $UF_4(H_2O)_{2.5}$.[11] Product yield declined with mixing beyond 144 hours with eventual complete dissolution of the material at 168 hours.

1.3 Methods

1.3.1 Raman Spectroscopy

Micro-Raman spectra of crystalline samples were acquired on two separate commercial Raman spectrometers. Spectra were collected with a LabRam HR800 UV (Horiba Jobin-Yvon) spectrometer and with the InVia (Renishaw) Raman spectrometer. The LabRam is equipped with a Newton EMCCD (Andor 970N-UVB) detector with a 1600 x 200 pixel array and iDus (DU416A-LDC-DD) detector (785 nm laser only) with a 2000 x 256 pixel array; 16 microns pixel resolution. Laser excitations of 325, 457, 488, 514, and 785 nm were used during the Raman spectral acquisition. The resolution depends on the wavelength, binning, grating and other parameters. For the spectra acquired with the 514nm, the resolution was 4.2 cm-1. For the spectra acquired with the 325 nm, the resolution was 20 cm-1. The resolution was decreased due to large binning of 4 pixels in order to enhance signal to noise ratio. Labspec 5.78 software was used to control the spectrometer and detector. The software was also used to conduct data manipulations on the data. Micro-Raman spectra were also collected on a Renishaw InVia Raman spectrometer

coupled with two excitation lasers consisting of a diode source single mode λ = 785 nm, 50 mW, and Ar ion λ = 514 nm, 50 mW, lasers. The laser power used in these experiments ranged from 100 μW to 2 mW. The laser intensity at the sample was controlled with neutral density filters and the microscope objective selection (primarily 100x). The InVia possess automated beam steering optics, motorized components (Rayleigh slit; entrance slit; pinhole, diffraction gratings (either 1200 g/mm and 1800 g/mm)), 100 cm^{-1} Raman edge filters, plasma line rejection filters, and a UVDD CCD detector. The InVia was used to collect spectra on the $UF_4(H_2O)_{2.5}$ before the LabRam was used due to laser availability. The LabRam is more sensitive and greater selection of lasers to reduce fluorescence. The spectral bands in the IR spectra were analyzed with GRAMS AI.

Spectra were acquired at the same point or at different points within the material (different crystals). Different acquisition times were conducted from 1/2 hour to several hours. Figure 2 spectra were baseline corrected since a rising fluorescence was observed in the 50 to 2000 cm-1. In general, similar S/N were used during the acquisitions. All spectra in Figure 2 was collected with 120s integration time with 2 co-additions. Each spectrum was the addition of three sections. UF4(anhydrous) data was acquired a couple of years before the data for the hydrates and the high resolution spectra took several hours at 514 nm to complete.

1.3.2 Infrared Spectroscopy

A Nicolet 6700 Fourier transform infrared spectrometer equipped with an attenuated total reflectance (ATR) accessory and a DTGS detector was used to measure the IR spectra of the uranium-fluoride compounds. The spectra were measured with a 4 cm^{-1} resolution and a total of 128 spectra were co-added during the acquisition and were recorded in the 400 to the 4000 cm^{-1} spectral window. Note the spectral region 2000-2200 cm^{-1} demonstrates no measurable signal due to the diamond ATR accessory, which after background substrate possess little to no signal. The spectral bands in the IR spectra were analyzed with GRAMS AI.

1.3.3 Powder X-ray Diffraction

Powder X-ray diffraction (pXRD) measurements were acquired using a Rigaku Ultima IV powder X-ray diffractometer with a multi-sample changer attachment. X-rays were produced from a copper target at 40 kV and 44 mA. Scattered X-rays were detected using a D/teX Ultra semi-conductor detector with a Cu Kβ filter, with the tube/detector operated in the focusing beam (Bragg Brentano) method. On the incident side of the beam, the divergence slit was set at 2/3° and the divergence height limit slit at 10 mm while the scattering slit was set at 8.0 mm and the receiving slit was open on the diffracted side of the beam. The sample substrate was a 1-inch silicon disk cut along the (510) crystal plane to minimize background reflections. Paraffin wax was used to secure the UF_4 hydrate powder to the substrate. The 2θ scan range was from 10 - 60° at a scan rate of 0.5° per minute. Measurements were performed with a stationary sample holder. XRD scans were analyzed with PDXL (Rigaku). A qualitative analysis was performed using a peak search to match the experimental XRD pattern to the ICDD database of crystal and powder X-ray diffraction pattern using the peak intensity and peak position.[19]

1.3.4 Single Crystal X-ray Diffraction

X-ray intensity data were collected using a Bruker SMART APEX diffractometer utilizing Mo K_α radiation (λ = 0.71073 Å). Raw area detector data frames were processed using SAINT+ and an absorption correction was applied with SADABS.[20] The final reported unit cell parameters were

determine by least-squares refinement of a large array of reflections taken from each data set. The initial structural model was obtained by direct methods using SHELXS and the subsequent full-matrix least-squares refinements against F^2 and difference Fourier calculations were performed with SHELXTL.[21] The crystal structures were visualized by using CrystalMaker (v9.2.6) to plot the atomic positions and bonds based of the CIF obtained from the single-crystal structure solution.

1.4 **Results and Discussion**

The work presented herein combines XRD analyses with infrared and Raman spectroscopy to measure key spectral signatures related to the polymeric structure and water bonding in hydrated uranium fluoride crystals. Raman and IR spectra of anhydrous UF_4 were compared to the spectra of the hydrated analogs. GRAMS AI with Lorenztian peaks were used to identify overlapping bands in the spectra and to help compare the Raman spectra with the infrared spectra in the OH stretch and HOH bending regions. The Raman spectra in the short spectral region were not fit since we know the bands are a combination of many bands and is then a best guess to determine which bands coordinate to which bonds. Most bands were identified by the peak maximum. Ab initio calculations were tried for UF4 and failed. The calculations were too complex and expensive with and required many assumptions. 3Most of the samples were stable with laser power below 2 mW. With UF_4 materials, it is best to start with low laser power and acquisition times, and slowly increase power, before increasing acquisition times to increase signal to noise, while monitoring for changes in the Raman bands that could be attributed to photodegradation. In general, we start below 0.5 mW power.

1.4.1 Raman Spectra

Figures 1 and 2 show the Raman spectra of anhydrous UF_4 and the three hydrates. The spectra in Figure 1 were measured with a 514 nm laser wavelength and cover the 50 to 600 cm^{-1} spectral region. The spectra were characterized by a series of bands in this region as shown in Table 1. Approximately 16 bands exist in this region in the anhydrous UF_4 system (as previously reported[12]) with four intense bands located at 129, 167, 256, and 297 cm^{-1}. Spectral complexity was found to increase with the content of water in the crystal lattice with the UF_4 hydrates showing significant band congestion, likely due to new bonds from the chemical interaction between water molecules and fluorine in the system.

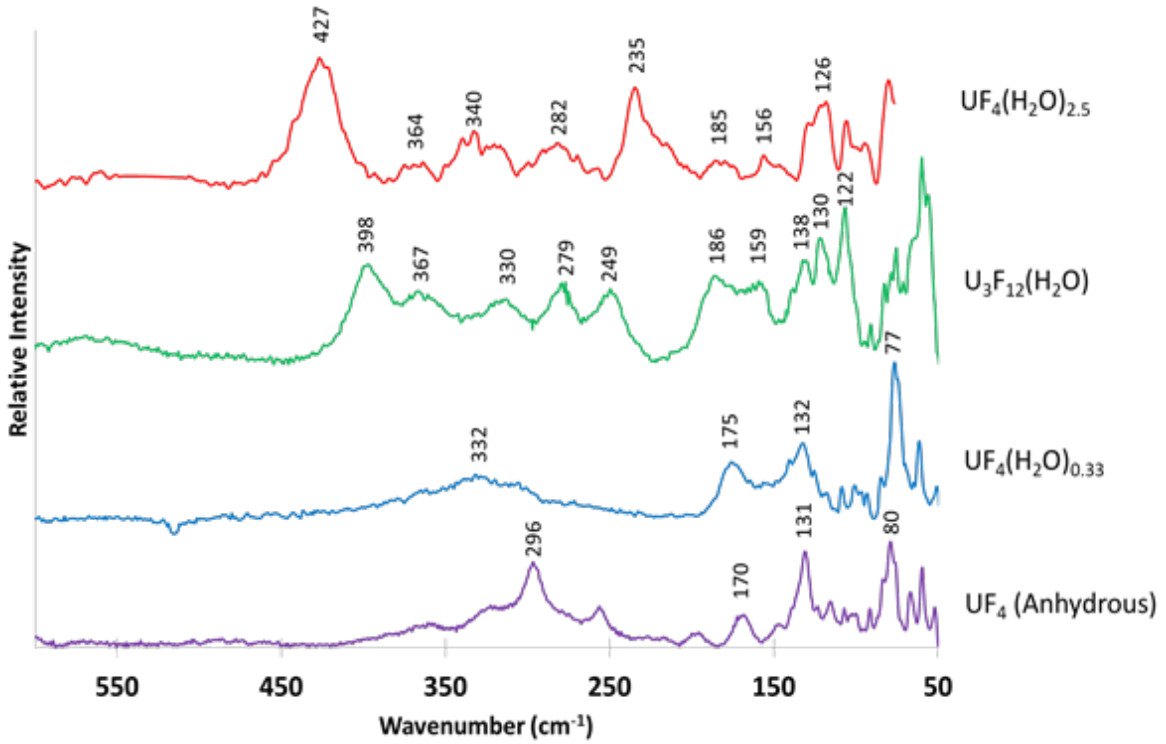

Figure 1: Raman of UF_4 anhydrous and UF_4 hydrates in order from top to bottom, $UF_4(H2O)_{2.5}$, $U_3F_{12}(H_2O)$, $UF_4(H_2O)_{0.33}$, and UF_4 anhydrous with the 514 nm laser.

Figure 2 shows the Raman spectra of UF_4 and the three hydrates acquired with the 325 nm laser. The 325 nm laser was primarily used to reduce the influence of fluorescence since the different compounds exhibited different fluorescence background and/or fluorescence intensity. The more common 785 nm laser did have decaying fluorescence with some samples; however, scattering was weak. Increasing power to increase signal has been shown to damage UF_4 samples. Another issue is that due to grating of 1800 grooves/mm, the spectrometer only allows the spectrometer to reach ~2800 cm^{-1}, with the OH stretch bands located beyond 3000 cm^{-1}. Specifically, with the 325 nm laser, two intense fluorescence bands were observed at 1600 cm^{-1} and at 500 cm^{-1} in both anhydrous UF_4 and the three hydrates. The intensity of the fluorescence bands decreased with water content suggesting fluorescence quenching and lifetime reduction. The absence of fluorescence with the 325 nm laser excitation line, (except for the bands just mentioned), provided a consistent, high-resolution means of acquiring the Raman spectra of UF_4 and the three hydrates. The complex polymeric structure of UF_4 and the hydrates was clearly identified via the phonons from numerous optical F-F vibrational modes in the lower wavenumber region (100 – 500 cm^{-1}), which were measured with a high signal to noise ratio.

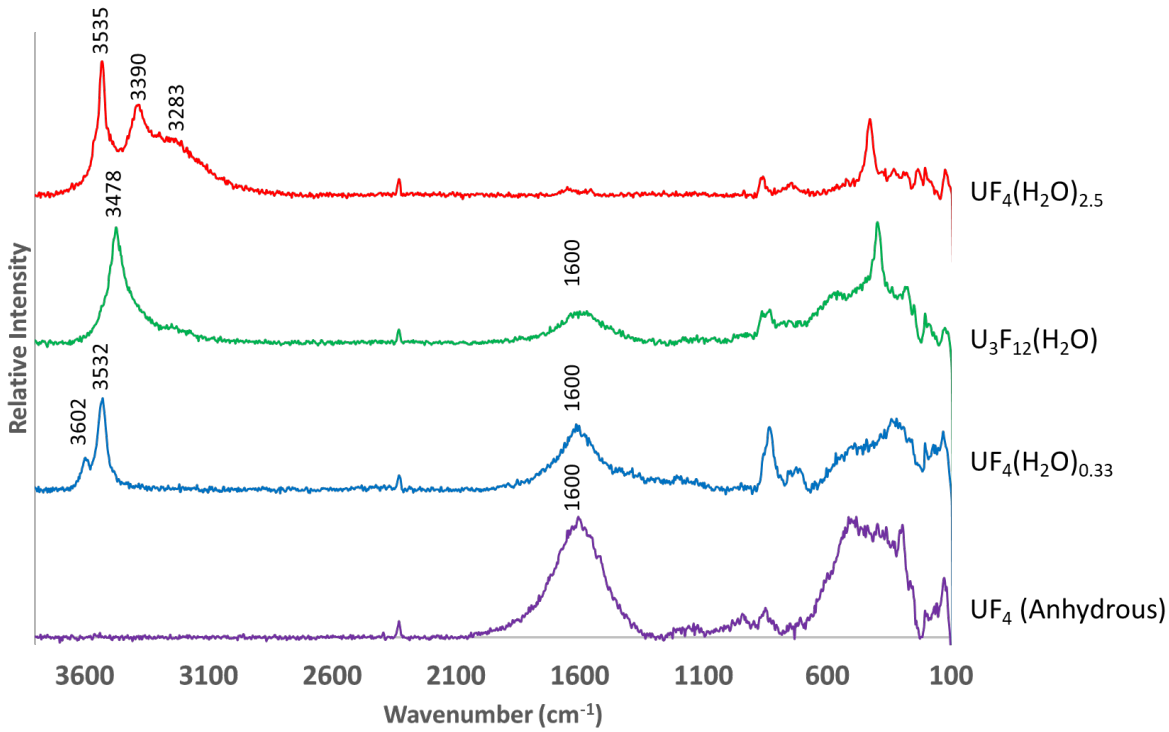

Figure 2: Complete Raman spectrum of each UF_4 hydrate hydrates in order from top to bottom, $UF_4(H2O)_{2.5}$, $U_3F_{12}(H_2O)$, $UF_4(H_2O)_{0.33}$, and UF_4 anhydrous with the 325 nm laser.

Overall, the OH spectral region (3000 – 3650 cm^{-1}) in Figure 2 can be described as an agglomerate of bands resulting from free and hydrogen bonded OH groups. Note, anhydrous UF_4 has no bands in this region, as is expected due to the lack of water in the crystal lattice. The typical vibrational spectrum of hydrogen bonded water consists of symmetric and asymmetric OH stretch modes since each OH can interact differently with its closest atomic neighbors. Chemical environment and selection rules for Raman and IR spectroscopy can affect the shape of the OH band and the number of bands in this region are indicative of the number of free and unique OH groups.

1.4.1.1 $UF_4(H_2O)_{2.5}$ Raman.

The Raman spectrum of $UF_4(H_2O)_{2.5}$ was markedly more complex relative to anhydrous UF_4 as shown in Figures 1 and 2. As shown in Table 1, with few exceptions, the Raman bands of $UF_4(H_2O)_{2.5}$ do not match the bands for anhydrous UF_4 or the other hydrate analogs. This result can be explained by the significant differences in crystal structures amongst the analyzed compounds. For example, UF_4 has a monoclinic unit cell with the C2/c space group, whereas $UF_4(H_2O)_{2.5}$ has a rhombic unit cell with Pnam space group. Clearly $UF_4(H_2O)_{2.5}$ has the most complex Raman spectrum of all the hydrates in the OH region (3000 – 3650 cm^{-1}); a result that is consistent with this compound having the highest hydration amongst the analyzed compounds. The crystal structure of $UF_4(H_2O)_{2.5}$ indicates there are UF_8, UF_9 and UF_5O_4 polyhedra and free water in the lattice.

The OH spectral region in the Raman spectrum was fitted with GRAMS AI. Four OH stretch bands were identified at 3535 (strong), 3481 (weak) 3390 (strong), and 3283 cm^{-1} (broad), with

FWHM of 42, 47, 77, and 312 cm^{-1}, respectively. The correlation number between the experimental data and the curve fit was 0.9949 with Std. Error. of 1.86. The higher standard error observed in the Raman spectrum curve fitting is mostly due to noise in the spectrum.

1.4.1.2 $UF_4(H_2O)_{0.33}$ Raman.

The Raman spectrum of $UF_4(H_2O)_{0.33}$ and anhydrous UF_4 have several bands in similar locations. Specifically, the $UF_4(H_2O)_{0.33}$ bands at 62, 77, 132, and 175 cm^{-1} mirror the bands of anhydrous UF_4. These are likely F-F phonons bands (transverse optical and longitudinal optical) and suggest $UF_4(H_2O)_{0.33}$ forms a UF_8 polyhedron in the crystalline lattice, similar to UF_4; a result that is confirmed by single crystal X-ray diffraction. The large fluorescence peak seen in anhydrous UF_4 at 1600 cm^{-1} is less intense in the $UF_4(H_2O)_{0.33}$ spectrum.

The Raman spectrum of $UF_4(H_2O)_{0.33}$ shows two bands in the OH stretching region. GRAMS AI identified the bands located at 3602 and 3533 cm^{-1} with FWHM of 34 and 39 cm^{-1}, respectively. The position and FWHM of these bands correspond to OH stretches that are free or mostly free from chemical interactions. The intensity of these bands might be related to the population in the crystal or symmetry rules.

1.4.1.3 $U_3F_{12}(H_2O)$ Raman.

$U_3F_{12}(H_2O)$ and $UF_4(H_2O)_{0.33}$ have identical stoichiometry, but different structures and therefore dissimilar vibrational spectra. The fluorescence intensity for $U_3F_{12}(H_2O)$ observed at 1600 cm^{-1} is weaker than the corresponding $UF_4(H_2O)_{0.33}$ but is still stronger than the band observed for the $UF_4(H_2O)_{2.5}$ hydrate. As previously stated, the intensity of fluorescence was observed to decrease with water content across the UF_4 hydrates, such that UF_4 has the most intense fluorescence band at 1600 cm^{-1} while $UF_4(H_2O)_{2.5}$ the weakest. The Raman spectrum of $U_3F_{12}(H_2O)$ is similar to the other hydrates in that it exhibits phonons from F-F transition bands at lower wavenumbers

The Raman OH stretch region for $U_3F_{12}(H_2O)$ was modeled with GRAMS AI and four bands were identified. These vibrational bands were located at 3532 (weak), 3478 (strong), 3405 (weak), and 3237 cm^{-1} (very weak) with FWHM of 42, 61, 124, and 91 cm^{-1}, respectively. Clearly, the spectrum is dominated by the band intense band at 3532 cm^{-1}. This band corresponds to a weakly hydrogen bonded OH group, thus indicating there may be a preferred OH site in the crystal lattice.

Table 1 Raman spectral peaks identified for UF_4 and the three hydrates. Peaks were identified using Grams AI fitting software. Peaks descriptions are: v, very; s, strong; m, medium; w, weak; br, broad; sh, shoulder.

UF_4		**$UF_4(H_2O)_{0.33}$**		**$U_3F_{12}{\cdot}H_2O$**		**$UF_4(H_2O)_{2.5}$**	
		3602	sh	3532	w	3535	s
		3532	s	3478	s	3480	w
				3405	w br	3390	m
				3237	w br	3283	m,s br
		637	w br	635	w		
604	w						
				569	w br		

						427	s
				398	m		
		382	w sh				
361	sh	363	sh	367	m	364	w
						340	m
		332	w br	330	w sh	333	m
322	sh					320	m sh
				314	m		
296	s	307	sh				
				279	m	282	m
256	m sh					257	w
				249	m		
						235	s br
197	w						
				186	m	185	w br
170	m	175	m				
				159	m	156	m br
149	sh						
		141	sh	138	s		
131	s	132	m	130	s		
		125	sh	122	s	126	m
116	w	118	sh				
107	w	108	w	106	s	118	m
						106	w
101	w sh br	102	w				
		96.8	sh br				
		93.3	w sh br			94.6	w
91	w			91	w		
		84.8	w	82.2	m sh	82	s
78.9	s	76.6	s	75.3	m sh		
				70.9	m		
66.8	m	61.7	m	63.7	s sh		
59.4	s			59.8	s sh		
		50.9	w				

1.4.2 Infrared Spectra

Infrared spectra of hydrogen bonded OH typically consist of a broad band centered around 3200 to 3550 cm^{-1}. Conversely, free OH functional groups, potentially sequestered due to steric effects, have limited interactions with nearby fluorine or water molecules and can result in sharp bands with FWHM <50 cm^{-1} in the 3590 to 3650 cm^{-1} spectral region. Therefore, the FWHM and location of the IR-active OH stretch is indicative of the chemical environment experienced in the crystal lattice.

The IR-active HOH bending mode provides information on the types of water molecules available in the crystal lattice. The number of these bands or the FWHM provides insight into the chemical

environments experienced by water molecules. In a crystal lattice, water molecules diffuse to different sites with low potential energy giving rise to different HOH bending modes.

In contrast to the free OH stretch that shifts to higher frequencies with decreased hydrogen bonding, the HOH bending mode shifts to lower frequencies for water molecules that experience minimal chemical interactions. The combination of the HOH bending mode frequencies with the type of OH stretch frequency and FWHM can help identify the sites in the crystal with water molecules. The band properties can be used to provide unique information on the metal bonding and the water content in the crystal lattice and the degree of crystallinity of the material.

Figures 3 and 4 show the IR spectra of anhydrous UF_4 and the three hydrates. The spectra were characterized by a series of bands as shown in Table 2.

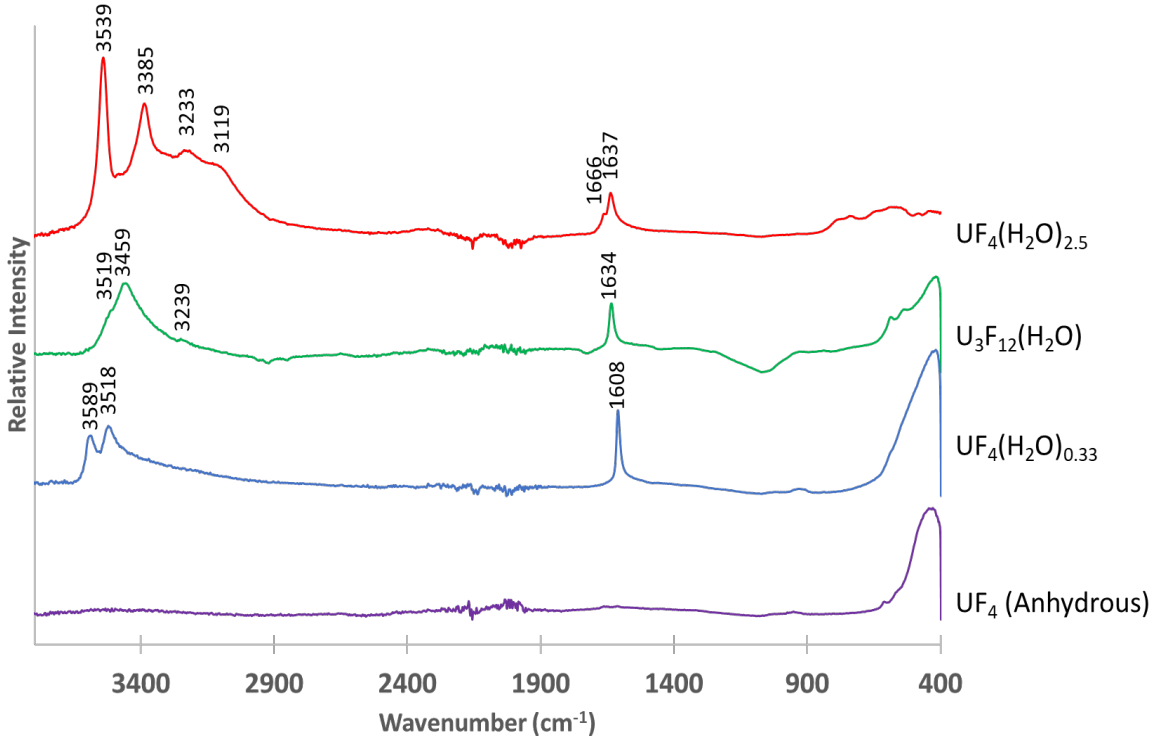

Figure 3: IR spectrum of each UF_4 hydrate hydrates in order from top to bottom, $UF_4(H2O)_{2.5}$, $U_3F_{12}(H_2O)$, $UF_4(H_2O)_{0.33}$, and UF_4 anhydrous

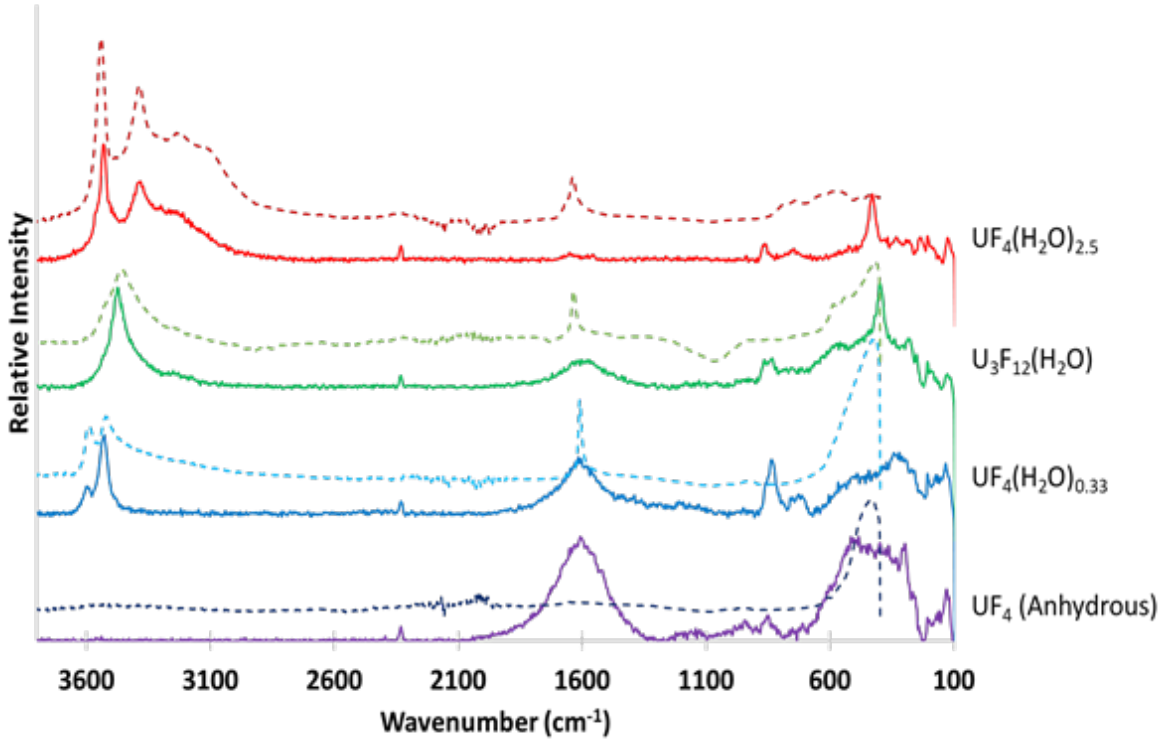

Figure 4: IR and Raman together to showcase the difference in the OH stretching region and HOH bending region. Raman spectra measured with the 325 nm. Dashed line = IR, Solid line = Raman

1.4.2.1 $UF_4(H_2O)_{2.5}$ Infrared.

1.4.2.1.1 High Frequencies (OH Stretch Modes)

Using the bands identified in the Raman of $UF_4(H_2O)_{2.5}$ as a guide, GRAMS AI identified 6 bands in the OH stretch region of the IR spectrum of $UF_4(H_2O)_{2.5}$. The program provided a good a fit for the entire OH stretch envelope. The bands that provided the best fit to the curve were 3539, 3470, 3385, 3283, 3218, and 3117 cm^{-1} with a FWHM of 42, 76, 87, 223, 80, and 245 cm^{-1}, respectively. The fit of the curve had a correlation number of 0.9946 with Std. Error. of 0.0008489. The sharp band at located at 3539 cm^{-1} is most likely a free OH stretch in the crystal lattice since free OH bands shift to higher frequencies relative to hydrogen bonded stretch modes. The rest of the bands in the OH stretching region are hydrogen bound with oxygen or fluorine, which leads to broadening and energy shifts.

1.4.2.1.2 Mid-Frequencies (HOH Bending Modes)

Three IR bands of $UF_4(H_2O)_{2.5}$ were observed at 1666, 1637 cm^{-1}, and 1599 cm^{-1}; these were used to fit the HOH bending region. The FWHM for the 1666, 1637, and 1599 cm^{-1} are 16, 31, and 116 cm^{-1}, respectively. Three HOH modes imply three different water molecules in the crystal lattice and agrees with the six bands observed in the OH stretch region.

1.4.2.1.3 Low Frequencies

GRAMS AI identified several low frequency bands in the IR spectrum of $UF_4(H_2O)_{2.5}$. These bands were located at 790, 737, 640, 590, 547, 489, and 423 cm^{-1}. The FWHM of the bands were modeled to be 61, 79, 114, 25, 84, 30, 129 cm^{-1}, respectively. The bands are most likely the result

of new bonds formed during the hydrogen bonding due to the three water molecules in the unit cell of this system.

1.4.2.2 $UF_4(H_2O)_{0.33}$ Infrared.

1.4.2.2.1 High Frequencies (OH Stretch Modes)

The IR spectrum $UF_4(H_2O)_{0.33}$ shows two strong bands in the high frequency range with a background that drifts slightly at lower frequencies. These bands were fitted with GRAMS AI to resolve the several bands of 3590, 3519, 3431, and 3238 $cm^{-1}$with a FWHM of 30, 65, 175, and 486 cm^{-1}, respectively. The band at 3590 cm^{-1} is most likely a free OH stretch vibration while the 3519 cm^{-1} has a weak interaction with the neighbors.

These two OH stretch bands bands suggests that although there is primarily one fixed water in the system, the tail of the OH stretch vibration agrees with the tail of the HOH bonding mode. The band at 3590 cm^{-1} suggests the OH bond is isolated from further interactions in the UF_4 while the band at 3519 cm^{-1} suggests very minor interaction in the crystal lattice whether with an oxygen or fluorine atom.

The bands at 3431 and 3237 cm^{-1} are possibly residual water in different locations in the crystal lattice. These bands are missing in the Raman spectrum suggesting that these bands are asymmetric vibrations (symmetric vibrations are strong in Raman spectroscopy while asymmetric vibrations are weak). The bands could also be missing due to a small scattering cross section or low polarizability.

1.4.2.2.2 Mid-Frequencies (HOH Bending Modes)

The HOH bending peak in the IR of $UF_4(H_2O)_{0.33}$ is indicated by an intense sharp band located at 1608 cm^{-1} with a FWHM of 15 cm^{-1} and a broad tail centered at 1556 cm^{-1} with a FWHM of 154 cm^{-1}. The narrow band suggest some water in $UF_4(H_2O)_{0.33}$ exists in a single chemical environment, whereas the band with the large FWHM suggests some water may exist in different states with different chemical interactions with oxygen and fluorine, thus creating a range of numerous configurations in the crystal.

1.4.2.3 $U_3F_{12}(H_2O)$ Infrared.

1.4.2.3.1 High Frequencies (OH Stretch Modes)

The IR spectrum of $U_3F_{12}(H_2O)$ shows a multi-structure "single" OH stretch band in the Raman and infrared spectra. Closer inspection of the multi-structure infrared OH stretch band with GRAMS AI shows the presence of four bands. The multi-band OH stretch can be modeled with a weak shoulder at 3520 cm^{-1}, a strong band at 3460 cm^{-1}, and two broad bands located at 3392 and 3240 cm^{-1} with FWHM of 50, 84, 137, and 329 cm^{-1}, respectively. In contrast to the other hydrates, no additional bands were required to fit the curve, although significant differences in band intensity for the 3392 and 3240 cm^{-1} were observed between the Raman and infrared spectra.

1.4.2.3.2 Mid-Frequencies (HOH Bending Modes)

The HOH bending mode contains two bands consisting of one strong sharp band located at 1634 cm^{-1} and one weak tail located at 1587 cm^{-1}. The bands located at 1634 and 1587 cm^{-1} have FWHM of 20.9 and 155 cm^{-1}, respectively.

1.4.2.3.3 Low Frequencies

Four additional bands were identified in the long wave infrared spectral region. The bands located at 588, 540, 435, and 413 cm^{-1} have FWHM of 39, 54, 174, and 33 cm^{-1}, respectively.

Table 2 IR spectral peaks for the three hydrates as characterized by attenuated total reflectance measurements and categorized based on likely vibrational mode identities. Bands were identified using Grams AI fitting software.

	$UF_4(H_2O)_{0.33}$	**$U_3F_{12}(H_2O)$**	**$UF_4(H_2O)_{2.5}$**	
			Khanaev et al. [22]	This work
O-H	3589 s		3540	3539 s
	3518 s	3519 w		
	3431 m br	3459 s		3470 w
		3392 br	3385	3385 s
				3313 br
	3237 br	3239 br	3230	3233 w br
			3110	3119 br
H_2O			1655	1666 w
		1634 s	1634	1637 s
	1608 s	1587 br	1600	1599 br
	1556 br			
H_2O/F				789 br
				737 br
			645	639 br
		587 w		589 br
			550	547 br
		540 w		
				485 br
	427 w	434 s	430	439 br
U-F		411 w		
	400 w		400	404 br

1.4.3 Powder X-ray diffraction and single crystal X-ray diffraction, Modeling and IR Data

Additional information on the type of water and chemical environment in the crystal lattice can be obtained with powder and single crystal X-ray diffraction. These techniques are invaluable, complementary tools in describing the vibrational spectroscopy of the UF_4 hydrates. Powder X-ray diffraction can help identify the molecular species in the crystal lattice such as the speciation of the hydrates while single crystal X-ray diffraction provides atom position and distances. The position of the uranium and oxygen atoms for UF_4 and the full crystalline cell obtained with single-crystal X-ray diffraction for UF_4 and the hydrates is shown in Figure 5.

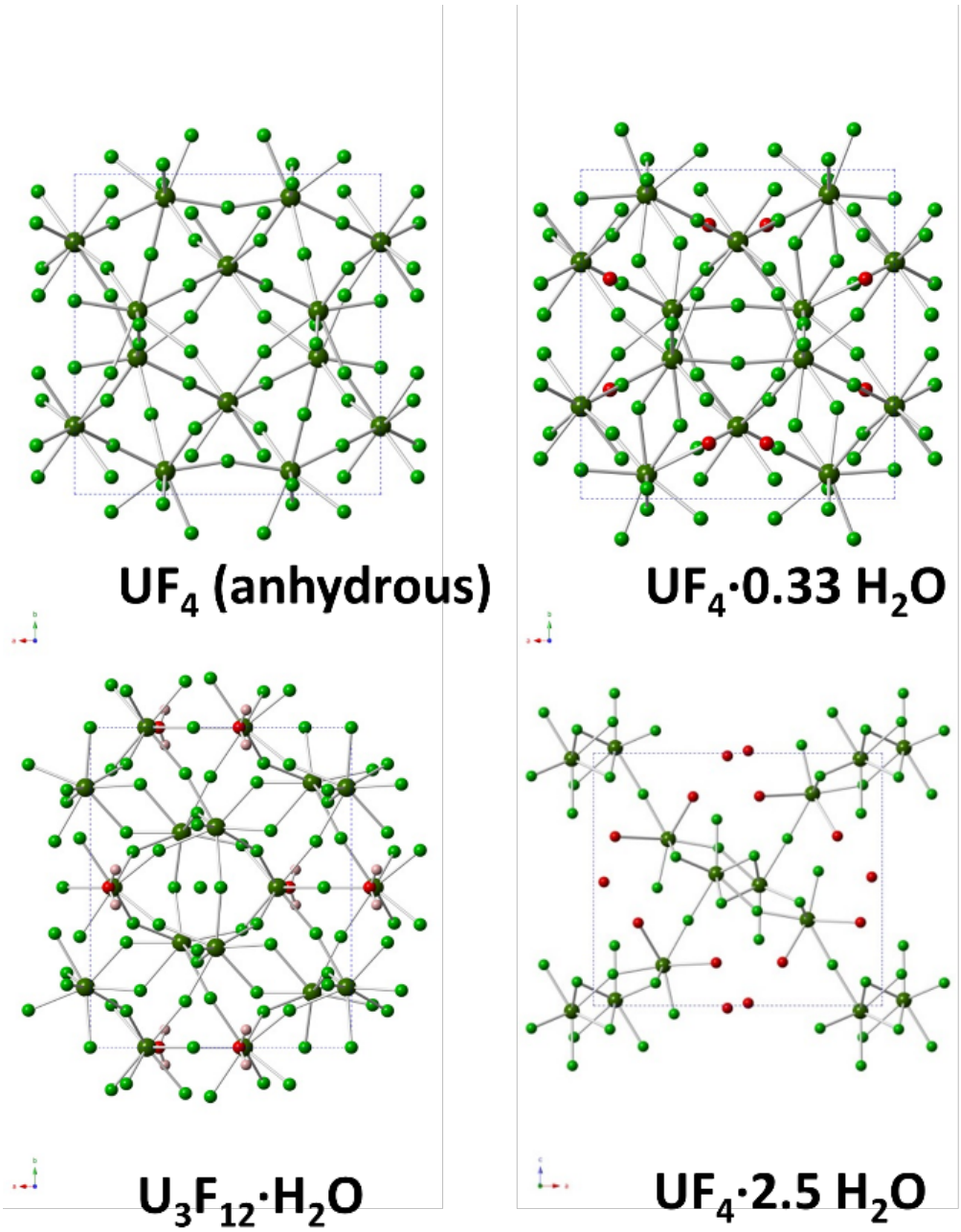

Figure 5: Crystallographic ball and stick diagram representations for anhydrous UF_4 and the three hydrates within a single unit cell. Gray = Uranium, Green = Fluorine, Red = Oxygen. Hydrogen atoms have been omitted for clarity.

1.4.3.1 $UF_4(H_2O)_{2.5}$

Single crystal XRD shows three waters in the crystal lattice of $UF_4(H_2O)_{2.5}$; one interstitial, and two bonded to uranium atoms. Zadneprovskii described that there are hydrogen bonds at O_2-H-F and O_3-H-F due to their reduced distances of 2.51 and 2.70 Å, respectively[11]. The shorter distance bond should manifest in vibrational spectra at a lower wavenumber than the longer distance bond. Other hydrogen bonding is possible from hydrogens O_2 and O_3 to the interstitial oxygen (O_1),

which are the same distance apart at 2.79Å. We postulate that these hydrogen bonds likely account for the six bands observed in the OH stretching region of the IR of $UF_4(H_2O)_{2.5}$ (see Table 2). The bands are likely broadened due to equivalent water molecules interacting with each other, possibly as dimers.

The HOH bending region in IR showed two distinguishable bands (1666 and 1637 cm^{-1}) and one delocalized tailing band. These bands can be attributed to there being at least three non-equivalent water molecules in the crystal lattice, which is consistent with the $UF_4(H_2O)_{2.5}$ crystal structure. The large FWHM of the tailing band is most likely related to water delocalization where the bending vibrational mode is located in many sites with largely different chemical environments.

Interstitial water found in the crystal structure of $UF_4(H_2O)_{2.5}$ is evidenced spectroscopically in the IR at 3539 cm^{-1} (the sharpest peak in the spectrum) and 1637 cm^{-1} (the HOH band). Comparative analysis of XRD and the IR spectrum seems to further indicate there are 3 water molecules in this lattice with the OH of two molecules bound to a uranium atom with different chemical environments and another OH of one molecule hydrogen bonded to another water molecule.

1.4.3.2 $UF_4(H_2O)_{0.33}$

XRD measurements of $UF_4(H_2O)_{0.33}$ indicate there is one water molecule in its unit cell. Raman of this compound showed two features identified as OH stretch bands at 3602 and 3533 cm^{-1}. The band located at 3602 cm^{-1} is identified as a free OH stretch while the band at 3533 cm^{-1} is due to OH with a minor interaction with its environment as indicated by the lower frequency and broader FWHM. These subtly different OH stretches are likely due to different distances between oxygen and its nearest fluorine and the F-O-U angle; a result that is consistent with the crystal structure.

In contrast to the XRD and Raman which indicate a single water molecule is present in a unit cell, the infrared spectrum of $UF_4(H_2O)_{0.33}$ indicates the presence of a second water molecule. The infrared spectrum shows similar bands as seen in Raman but the sharp bands are superimposed on a much broader background. This broad background in the IR corresponds to a hydrogen bonded OH. This data suggests that the IR bands at 3431 and 3237 cm^{-1} are asymmetric, which results in weak intensity in the Raman spectrum, hence why they were not observed via Raman.

The rationale for the difference in the XRD and IR results (i.e., the presence of one water molecule in XRD and two in IR) is currently unclear. Nonetheless, evidence for two water molecules is further supposed by the HOH bending mode (1608 cm^{-1}) in the IR of $UF_4(H_2O)_{0.33}$ and a tail in the spectrum at 1556 cm^{-1}. These are likely due to HOH participating in hydrogen bonding in the crystal lattice, which is not strongly supported by the XRD-derived crystal structure.

1.4.3.3 $U_3F_{12}(H_2O)$

Unlike $UF_4(H_2O)_{0.33}$, XRD of $U_3F_{12}(H_2O)$ identified two water molecules in the unit cell. According to the XRD data, the water molecules in $U_3F_{12}(H_2O)$ have a preferred location in the crystal lattice where both OH's in the water molecules have similar H-F distance and F-H-O bond angles. However, the IR and Raman spectra of $U_3F_{12}(H_2O)$ suggest the water molecules may not be identical. The OH IR region of $U_3F_{12}(H_2O)$ can be resolved into four bands as shown in Table 2. These band positions indicate there is a free OH, a quasi-free OH, and two hydrogen bonded OH's in the structure of $U_3F_{12}(H_2O)$. The Raman spectra of $U_3F_{12}(H_2O)$ shows something similar,

in that a broad OH stretch was found to consistent of four bands as shown in Table 1. These Raman band positions indicate there is selectivity for symmetric stretch bands and the F-H-O bond is likely affecting the FWHM resulting in a narrower band than typically observed from intermolecular water hydrogen bonds. Thus, the XRD data showing two identical water molecules is in contrast with both the IR and Raman data. The hydrogen positions measured via XRD could be the driving factor as to why the XRD and the vibrational spectra do not match, as crystallographers will generally take hydrogen locations as an absolute position, which is not necessarily true.

1.5 Summary

The Raman and IR spectra for three UF_4 hydrates are reported for the first time. Each hydrate has similar but complex Raman bands at low wavenumbers corresponding to optical phonons of polymeric F-F structural motifs, thus highlighting the similar UF_x polyhedral networks that can exist in the different hydrate lattices. The OH stretch and HOH bending modes of these compounds, in conjunction with XRD data, helped provide a new perspective on water molecules in the three different compounds. The greatest difference between these three hydrates is seen in the OH stretching region of the IR where band locations and FWHM of bands vary by compound. Both anhydrous UF_4 and the three hydrates exhibited varying fluorescence intensities, that decreased with stoichiometric water content both at low wavenumbers, and at ~1600 cm^{-1} spectral region. XRD results in general agree with the data acquired from the vibrational spectra.

1.6 Acknowledgements

The authors would like to think Dr. Jonathan Christian for helping with scientific discussions, Michael Summer for his contributing efforts on the collection of SEM images, Ross Smith for his assistance with Raman spectral collection, Dr. Maria Kriz for her insight on the collection and analysis of XRD data, Dr. Marine Duff for her insight on experimental design, and the staff of International Bioanalytical Laboratories for their technical discussions on uranium synthesis. The United States Government retains and the publisher, by accepting this article for publication, acknowledges that the United States Government retains a nonexclusive, paid-up, irrevocable, worldwide license to publish or reproduce the published form of this work, or to allow others to do so, for United States Government purposes.

1.7 Funding

This work was funded by the U.S. Department of Energy, Savannah River National Laboratory Research and Development program, under project #LDRD-2016-00031 and by the U.S. Department of Energy, Office of Basic Energy Sciences, Division of Materials Sciences and Engineering under Award DE-SC00018739.

References

(1) Gorden, A. E. V.; DeVore, M. A.; Maynard, B. A. *Inorg. Chem.* **2013**, *52*, 3445.

(2) Maynard, B. A.; Lynn, K. S.; Sykora, R. E.; Gorden, A. E. V. *Inorg. Chem.* **2013**, *52*, 4880.

(3) Yeon, J.; Smith, M. D.; Sefat, A. S.; Tran, T. T.; Halasyamani, P. S.; zur Loye, H.-C. *Inorg. Chem.* **2013**, *52*, 8303.

(4) Yeon, J.; Smith, M. D.; Tapp, J.; Moller, A.; zur Loye, H.-C. *Inorg. Chem.* **2014**, *53*, 6289.

(5) Yeon, J.; Smith, M. D.; Tapp, J.; Moller, A.; zur Loye, H.-C. *J. Am. Chem. Soc.* **2014**, *136*, 3955.

(6) Felder, J.; Yeon, J.; Smith, M.; zur Loye, H.-C. *Inorg. Chem. Front.* **2017**, *4*, 368.

(7) Yashenko, K. *Isvest. Akad. Nauk, U.S.S.R., Otdel. Khim. Nauk* **1942**, *87*.

(8) Dawson, J. K.; D'Eye, R. W. M.; Truswell, A. E. *Journal of the Chemical Society (Resumed)* **1954**, 3922.

(9) Gabuda, S. P. M., A.A.; Zadneprovskii, G.M. *Zhurnal Struknumoi Khimii* **1969**, *10*, 1115.

(10) Gagarinskii, Y. V. K., E.I.; Galkin, N.P.; Anan'eva, L.A.; Gabuda, S.P *Atomnaya Energiya* **1965**, *18*, 40.

(11) Zadneprovskii, G. M. B., S.V. *Zhurnal Struknumoi Khimii* **1971**, *12*, 831.

(12) Villa-Aleman, E.; Wellons, M. S. *Journal of Raman Spectroscopy* **2016**, *47*, 865.

(13) Miskowiec, A.; Shields, A. E.; Niedziela, J. L.; Cheng, Y.; Taylor, P.; DelCul, G.; Hunt, R.; Spencer, B.; Langford, J.; Abernathy, D. *Physica B: Condensed Matter* **2019**, *570*, 194.

(14) Villa-Aleman, E., Wellons, M.S. *JRSp* **2016**, *47*, 865.

(15) Kern, S.; Hayward, J.; Roberts, S.; Jr., J. W. R.; Rotella, F. J.; Soderholm, L.; Cort, B.; Tinkle, M.; West, M.; Hoisington, D.; Lander, G. H. *The Journal of Chemical Physics* **1994**, *101*, 9333.

(16)

(17) Larson, A. C.; Roof, R. B., Jnr; Cromer, D. T. *Acta Crystallogr.* **1964**, *17*, 555.

(18) Yeon, J. S., Mark D.; Sefat, Athena, S.; Tran, T. Thao; Halasyamani, P. Shiv; Zur Loye, Hans-Conrad *Inorg. Chem.* **2013**, *52*, 8303.

(19) Gates-Rector, S.; Blanton, T. *Powder Diffraction* **2019**, *34*, 352.

(20) Huebschle, C. B.; Sheldrick, G. M.; Dittrich, B. *J. Appl. Crystallogr.* **2011**, *44*, 1281.

(21) Sheldrick, G. M. *Acta Crystallogr., Sect. A: Found. Crystallogr.* **2008**, *64*, 112.

(22) Khanaev, E. I.; Teterin, E. G.; Luk'yanova, L. A. *Journal of Applied Spectroscopy* **1967**, *6*, 533.